FERMILAB-PUB-11-021-E

Search for the Higgs boson in the all-hadronic final state using the CDF II detector

T. Aaltonen,[21] B. Álvarez González[v],[9] S. Amerio,[41] D. Amidei,[32] A. Anastassov,[36] A. Annovi,[17] J. Antos,[12] G. Apollinari,[15] J.A. Appel,[15] A. Apresyan,[46] T. Arisawa,[56] A. Artikov,[13] J. Asaadi,[51] W. Ashmanskas,[15] B. Auerbach,[59] A. Aurisano,[51] F. Azfar,[40] W. Badgett,[15] A. Barbaro-Galtieri,[26] V.E. Barnes,[46] B.A. Barnett,[23] P. Barria[cc],[44] P. Bartos,[12] M. Bauce[aa],[41] G. Bauer,[30] F. Bedeschi,[44] D. Beecher,[28] S. Behari,[23] G. Bellettini[bb],[44] J. Bellinger,[58] D. Benjamin,[14] A. Beretvas,[15] A. Bhatti,[48] M. Binkley,[15] D. Bisello[aa],[41] I. Bizjak[gg],[28] K.R. Bland,[5] B. Blumenfeld,[23] A. Bocci,[14] A. Bodek,[47] D. Bortoletto,[46] J. Boudreau,[45] A. Boveia,[11] B. Brau[a],[15] L. Brigliadori[z],[6] A. Brisuda,[12] C. Bromberg,[33] E. Brucken,[21] M. Bucciantonio[bb],[44] J. Budagov,[13] H.S. Budd,[47] S. Budd,[22] K. Burkett,[15] G. Busetto[aa],[41] P. Bussey,[19] A. Buzatu,[31] C. Calancha,[29] S. Camarda,[4] M. Campanelli,[33] M. Campbell,[32] F. Canelli[12],[15] A. Canepa,[43] B. Carls,[22] D. Carlsmith,[58] R. Carosi,[44] S. Carrillo[k],[16] S. Carron,[15] B. Casal,[9] M. Casarsa,[15] A. Castro[z],[6] P. Catastini,[15] D. Cauz,[52] V. Cavaliere[cc],[44] M. Cavalli-Sforza,[4] A. Cerri[f],[26] L. Cerrito[q],[28] Y.C. Chen,[1] M. Chertok,[7] G. Chiarelli,[44] G. Chlachidze,[15] F. Chlebana,[15] K. Cho,[25] D. Chokheli,[13] J.P. Chou,[20] W.H. Chung,[58] Y.S. Chung,[47] C.I. Ciobanu,[42] M.A. Ciocci[cc],[44] A. Clark,[18] G. Compostella[aa],[41] M.E. Convery,[15] J. Conway,[7] M.Corbo,[42] M. Cordelli,[17] C.A. Cox,[7] D.J. Cox,[7] F. Crescioli[bb],[44] C. Cuenca Almenar,[59] J. Cuevas[v],[9] R. Culbertson,[15] D. Dagenhart,[15] N. d'Ascenzo[t],[42] M. Datta,[15] P. de Barbaro,[47] S. De Cecco,[49] G. De Lorenzo,[4] M. Dell'Orso[bb],[44] C. Deluca,[4] L. Demortier,[48] J. Deng[c],[14] M. Deninno,[6] F. Devoto,[21] M. d'Errico[aa],[41] A. Di Canto[bb],[44] B. Di Ruzza,[44] J.R. Dittmann,[5] M. D'Onofrio,[27] S. Donati[bb],[44] P. Dong,[15] M. Dorigo,[52] T. Dorigo,[41] K. Ebina,[56] A. Elagin,[51] A. Eppig,[32] R. Erbacher,[7] D. Errede,[22] S. Errede,[22] N. Ershaidat[y],[42] R. Eusebi,[51] H.C. Fang,[26] S. Farrington,[40] M. Feindt,[24] J.P. Fernandez,[29] C. Ferrazza[dd],[44] R. Field,[16] G. Flanagan[r],[46] R. Forrest,[7] M.J. Frank,[5] M. Franklin,[20] J.C. Freeman,[15] Y. Funakoshi,[56] I. Furic,[16] M. Gallinaro,[48] J. Galyardt,[10] J.E. Garcia,[18] A.F. Garfinkel,[46] P. Garosi[cc],[44] H. Gerberich,[22] E. Gerchtein,[15] S. Giagu[ee],[49] V. Giakoumopoulou,[3] P. Giannetti,[44] K. Gibson,[45] C.M. Ginsburg,[15] N. Giokaris,[3] P. Giromini,[17] M. Giunta,[44] G. Giurgiu,[23] V. Glagolev,[13] D. Glenzinski,[15] M. Gold,[35] D. Goldin,[51] N. Goldschmidt,[16] A. Golossanov,[15] G. Gomez,[9] G. Gomez-Ceballos,[30] M. Goncharov,[30] O. González,[29] I. Gorelov,[35] A.T. Goshaw,[14] K. Goulianos,[48] A. Gresele,[41] S. Grinstein,[4] C. Grosso-Pilcher,[11] R.C. Group,[55] J. Guimaraes da Costa,[20] Z. Gunay-Unalan,[33] C. Haber,[26] S.R. Hahn,[15] E. Halkiadakis,[50] A. Hamaguchi,[39] J.Y. Han,[47] F. Happacher,[17] K. Hara,[53] D. Hare,[50] M. Hare,[54] R.F. Harr,[57] K. Hatakeyama,[5] C. Hays,[40] M. Heck,[24] J. Heinrich,[43] M. Herndon,[58] S. Hewamanage,[5] D. Hidas,[50] A. Hocker,[15] W. Hopkins[g],[15] D. Horn,[24] S. Hou,[1] R.E. Hughes,[37] M. Hurwitz,[11] U. Husemann,[59] N. Hussain,[31] M. Hussein,[33] J. Huston,[33] G. Introzzi,[44] M. Iori[ee],[49] A. Ivanov[o],[7] E. James,[15] D. Jang,[10] B. Jayatilaka,[14] E.J. Jeon,[25] M.K. Jha,[6] S. Jindariani,[15] W. Johnson,[7] M. Jones,[46] K.K. Joo,[25] S.Y. Jun,[10] T.R. Junk,[15] T. Kamon,[51] P.E. Karchin,[57] Y. Kato[n],[39] W. Ketchum,[11] J. Keung,[43] V. Khotilovich,[51] B. Kilminster,[15] D.H. Kim,[25] H.S. Kim,[25] H.W. Kim,[25] J.E. Kim,[25] M.J. Kim,[17] S.B. Kim,[25] S.H. Kim,[53] Y.K. Kim,[11] N. Kimura,[56] M. Kirby,[15] S. Klimenko,[16] K. Kondo,[56] D.J. Kong,[25] J. Konigsberg,[16] A.V. Kotwal,[14] M. Kreps,[24] J. Kroll,[43] D. Krop,[11] N. Krumnack[l],[5] M. Kruse,[14] V. Krutelyov[d],[51] T. Kuhr,[24] M. Kurata,[53] S. Kwang,[11] A.T. Laasanen,[46] S. Lami,[44] S. Lammel,[15] M. Lancaster,[28] R.L. Lander,[7] K. Lannon[u],[37] A. Lath,[50] G. Latino[cc],[44] I. Lazzizzera,[41] T. LeCompte,[2] E. Lee,[51] H.S. Lee,[11] J.S. Lee,[25] S.W. Lee[w],[51] S. Leo[bb],[44] S. Leone,[44] J.D. Lewis,[15] C.-J. Lin,[26] J. Linacre,[40] M. Lindgren,[15] E. Lipeles,[43] A. Lister,[18] D.O. Litvintsev,[15] C. Liu,[45] Q. Liu,[46] T. Liu,[15] S. Lockwitz,[59] N.S. Lockyer,[43] A. Loginov,[59] D. Lucchesi[aa],[41] J. Lueck,[24] P. Lujan,[26] P. Lukens,[15] G. Lungu,[48] J. Lys,[26] R. Lysak,[12] R. Madrak,[15] K. Maeshima,[15] K. Makhoul,[30] P. Maksimovic,[23] S. Malik,[48] G. Manca[b],[27] A. Manousakis-Katsikakis,[3] F. Margaroli,[46] C. Marino,[24] M. Martínez,[4] R. Martínez-Ballarín,[29] P. Mastrandrea,[49] M. Mathis,[23] M.E. Mattson,[57] P. Mazzanti,[6] K.S. McFarland,[47] P. McIntyre,[51] R. McNulty[i],[27] A. Mehta,[27] P. Mehtala,[21] A. Menzione,[44] C. Mesropian,[48] T. Miao,[15] D. Mietlicki,[32] A. Mitra,[1] H. Miyake,[53] S. Moed,[20] N. Moggi,[6] M.N. Mondragon[k],[15] C.S. Moon,[25] R. Moore,[15] M.J. Morello,[15] J. Morlock,[24] P. Movilla Fernandez,[15] A. Mukherjee,[15] Th. Muller,[24] P. Murat,[15] M. Mussini[z],[6] J. Nachtman[m],[15] Y. Nagai,[53] J. Naganoma,[56] I. Nakano,[38] A. Napier,[54] J. Nett,[51] C. Neu,[55] M.S. Neubauer,[22] J. Nielsen[e],[26] L. Nodulman,[2] O. Norniella,[22] E. Nurse,[28] L. Oakes,[40] S.H. Oh,[14] Y.D. Oh,[25] I. Oksuzian,[55] T. Okusawa,[39] R. Orava,[21] L. Ortolan,[4] S. Pagan Griso[aa],[41] C. Pagliarone,[52] E. Palencia[f],[9] V. Papadimitriou,[15] A.A. Paramonov,[2] J. Patrick,[15] G. Pauletta[ff],[52] M. Paulini,[10] C. Paus,[30] D.E. Pellett,[7] A. Penzo,[52] T.J. Phillips,[14] G. Piacentino,[44] E. Pianori,[43] J. Pilot,[37] K. Pitts,[22] C. Plager,[8] L. Pondrom,[58] K. Potamianos,[46] O. Poukhov,[13] F. Prokoshin[x],[13] A. Pronko,[15] F. Ptohos[h],[17] E. Pueschel,[10] G. Punzi[bb],[44] J. Pursley,[58] A. Rahaman,[45] V. Ramakrishnan,[58] N. Ranjan,[46] I. Redondo,[29] P. Renton,[40] M. Rescigno,[49] F. Rimondi[z],[6] L. Ristori[45],[15] A. Robson,[19]

T. Rodrigo,[9] T. Rodriguez,[43] E. Rogers,[22] S. Rolli,[54] R. Roser,[15] M. Rossi,[52] F. Rubbo,[15] F. Ruffini[cc],[44] A. Ruiz,[9] J. Russ,[10] V. Rusu,[15] A. Safonov,[51] W.K. Sakumoto,[47] Y. Sakurai,[56] L. Santi[ff],[52] L. Sartori,[44] K. Sato,[53] V. Saveliev[t],[42] A. Savoy-Navarro,[42] P. Schlabach,[15] A. Schmidt,[24] E.E. Schmidt,[15] M.P. Schmidt,[59] M. Schmitt,[36] T. Schwarz,[7] L. Scodellaro,[9] A. Scribano[cc],[44] F. Scuri,[44] A. Sedov,[46] S. Seidel,[35] Y. Seiya,[39] A. Semenov,[13] F. Sforza[bb],[44] A. Sfyrla,[22] S.Z. Shalhout,[7] T. Shears,[27] P.F. Shepard,[45] M. Shimojima[s],[53] S. Shiraishi,[11] M. Shochet,[11] I. Shreyber,[34] A. Simonenko,[13] P. Sinervo,[31] A. Sissakian,[13] K. Sliwa,[54] J.R. Smith,[7] F.D. Snider,[15] A. Soha,[15] S. Somalwar,[50] V. Sorin,[4] P. Squillacioti,[15] M. Stancari,[15] M. Stanitzki,[59] R. St. Denis,[19] B. Stelzer,[31] O. Stelzer-Chilton,[31] D. Stentz,[36] J. Strologas,[35] G.L. Strycker,[32] Y. Sudo,[53] A. Sukhanov,[16] I. Suslov,[13] K. Takemasa,[53] Y. Takeuchi,[53] J. Tang,[11] M. Tecchio,[32] P.K. Teng,[1] J. Thom[g],[15] J. Thome,[10] G.A. Thompson,[22] E. Thomson,[43] P. Ttito-Guzmán,[29] S. Tkaczyk,[15] D. Toback,[51] S. Tokar,[12] K. Tollefson,[33] T. Tomura,[53] D. Tonelli,[15] S. Torre,[17] D. Torretta,[15] P. Totaro[ff],[52] M. Trovato[dd],[44] Y. Tu,[43] F. Ukegawa,[53] S. Uozumi,[25] A. Varganov,[32] F. Vázquez[k],[16] G. Velev,[15] C. Vellidis,[3] M. Vidal,[29] I. Vila,[9] R. Vilar,[9] J. Vizán,[9] M. Vogel,[35] G. Volpi[bb],[44] P. Wagner,[43] R.L. Wagner,[15] T. Wakisaka,[39] R. Wallny,[8] S.M. Wang,[1] A. Warburton,[31] D. Waters,[28] M. Weinberger,[51] W.C. Wester III,[15] B. Whitehouse,[54] D. Whiteson[c],[43] A.B. Wicklund,[2] E. Wicklund,[15] S. Wilbur,[11] F. Wick,[24] H.H. Williams,[43] J.S. Wilson,[37] P. Wilson,[15] B.L. Winer,[37] P. Wittich[g],[15] S. Wolbers,[15] H. Wolfe,[37] T. Wright,[32] X. Wu,[18] Z. Wu,[5] K. Yamamoto,[39] J. Yamaoka,[14] T. Yang,[15] U.K. Yang[p],[11] Y.C. Yang,[25] W.-M. Yao,[26] G.P. Yeh,[15] K. Yi[m],[15] J. Yoh,[15] K. Yorita,[56] T. Yoshida[j],[39] G.B. Yu,[14] I. Yu,[25] S.S. Yu,[15] J.C. Yun,[15] A. Zanetti,[52] Y. Zeng,[14] and S. Zucchelli[z6]

(CDF Collaboration)

[1] *Institute of Physics, Academia Sinica, Taipei, Taiwan 11529, Republic of China*
[2] *Argonne National Laboratory, Argonne, Illinois 60439, USA*
[3] *University of Athens, 157 71 Athens, Greece*
[4] *Institut de Fisica d'Altes Energies, ICREA, Universitat Autonoma de Barcelona, E-08193, Bellaterra (Barcelona), Spain*
[5] *Baylor University, Waco, Texas 76798, USA*
[6] *Istituto Nazionale di Fisica Nucleare Bologna, [z] University of Bologna, I-40127 Bologna, Italy*
[7] *University of California, Davis, Davis, California 95616, USA*
[8] *University of California, Los Angeles, Los Angeles, California 90024, USA*
[9] *Instituto de Fisica de Cantabria, CSIC-University of Cantabria, 39005 Santander, Spain*
[10] *Carnegie Mellon University, Pittsburgh, Pennsylvania 15213, USA*
[11] *Enrico Fermi Institute, University of Chicago, Chicago, Illinois 60637, USA*
[12] *Comenius University, 842 48 Bratislava, Slovakia; Institute of Experimental Physics, 040 01 Kosice, Slovakia*
[13] *Joint Institute for Nuclear Research, RU-141980 Dubna, Russia*
[14] *Duke University, Durham, North Carolina 27708, USA*
[15] *Fermi National Accelerator Laboratory, Batavia, Illinois 60510, USA*
[16] *University of Florida, Gainesville, Florida 32611, USA*
[17] *Laboratori Nazionali di Frascati, Istituto Nazionale di Fisica Nucleare, I-00044 Frascati, Italy*
[18] *University of Geneva, CH-1211 Geneva 4, Switzerland*
[19] *Glasgow University, Glasgow G12 8QQ, United Kingdom*
[20] *Harvard University, Cambridge, Massachusetts 02138, USA*
[21] *Division of High Energy Physics, Department of Physics, University of Helsinki and Helsinki Institute of Physics, FIN-00014, Helsinki, Finland*
[22] *University of Illinois, Urbana, Illinois 61801, USA*
[23] *The Johns Hopkins University, Baltimore, Maryland 21218, USA*
[24] *Institut für Experimentelle Kernphysik, Karlsruhe Institute of Technology, D-76131 Karlsruhe, Germany*
[25] *Center for High Energy Physics: Kyungpook National University, Daegu 702-701, Korea; Seoul National University, Seoul 151-742, Korea; Sungkyunkwan University, Suwon 440-746, Korea; Korea Institute of Science and Technology Information, Daejeon 305-806, Korea; Chonnam National University, Gwangju 500-757, Korea; Chonbuk National University, Jeonju 561-756, Korea*
[26] *Ernest Orlando Lawrence Berkeley National Laboratory, Berkeley, California 94720, USA*
[27] *University of Liverpool, Liverpool L69 7ZE, United Kingdom*
[28] *University College London, London WC1E 6BT, United Kingdom*
[29] *Centro de Investigaciones Energeticas Medioambientales y Tecnologicas, E-28040 Madrid, Spain*
[30] *Massachusetts Institute of Technology, Cambridge, Massachusetts 02139, USA*
[31] *Institute of Particle Physics: McGill University, Montréal, Québec, Canada H3A 2T8; Simon Fraser University, Burnaby, British Columbia, Canada V5A 1S6; University of Toronto, Toronto, Ontario, Canada M5S 1A7; and TRIUMF, Vancouver, British Columbia, Canada V6T 2A3*

[32] University of Michigan, Ann Arbor, Michigan 48109, USA
[33] Michigan State University, East Lansing, Michigan 48824, USA
[34] Institution for Theoretical and Experimental Physics, ITEP, Moscow 117259, Russia
[35] University of New Mexico, Albuquerque, New Mexico 87131, USA
[36] Northwestern University, Evanston, Illinois 60208, USA
[37] The Ohio State University, Columbus, Ohio 43210, USA
[38] Okayama University, Okayama 700-8530, Japan
[39] Osaka City University, Osaka 588, Japan
[40] University of Oxford, Oxford OX1 3RH, United Kingdom
[41] Istituto Nazionale di Fisica Nucleare, Sezione di Padova-Trento, [aa] University of Padova, I-35131 Padova, Italy
[42] LPNHE, Universite Pierre et Marie Curie/IN2P3-CNRS, UMR7585, Paris, F-75252 France
[43] University of Pennsylvania, Philadelphia, Pennsylvania 19104, USA
[44] Istituto Nazionale di Fisica Nucleare Pisa, [bb] University of Pisa,
[cc] University of Siena and [dd] Scuola Normale Superiore, I-56127 Pisa, Italy
[45] University of Pittsburgh, Pittsburgh, Pennsylvania 15260, USA
[46] Purdue University, West Lafayette, Indiana 47907, USA
[47] University of Rochester, Rochester, New York 14627, USA
[48] The Rockefeller University, New York, New York 10065, USA
[49] Istituto Nazionale di Fisica Nucleare, Sezione di Roma 1,
[ee] Sapienza Università di Roma, I-00185 Roma, Italy
[50] Rutgers University, Piscataway, New Jersey 08855, USA
[51] Texas A&M University, College Station, Texas 77843, USA
[52] Istituto Nazionale di Fisica Nucleare Trieste/Udine,
I-34100 Trieste, [ff] University of Trieste/Udine, I-33100 Udine, Italy
[53] University of Tsukuba, Tsukuba, Ibaraki 305, Japan
[54] Tufts University, Medford, Massachusetts 02155, USA
[55] University of Virginia, Charlottesville, VA 22906, USA
[56] Waseda University, Tokyo 169, Japan
[57] Wayne State University, Detroit, Michigan 48201, USA
[58] University of Wisconsin, Madison, Wisconsin 53706, USA
[59] Yale University, New Haven, Connecticut 06520, USA

(Dated: January 27, 2011)

We report on a search for the production of the Higgs boson decaying to two bottom quarks accompanied by two additional quarks. The data sample used corresponds to an integrated luminosity of approximately $4\,\mathrm{fb}^{-1}$ of $p\bar{p}$ collisions at $\sqrt{s} = 1.96\,\mathrm{TeV}$ recorded by the CDF II experiment. This search includes twice the data of the previous published result, uses new analysis techniques to distinguish jets originating from light flavor quarks and those from gluon radiation, and adds sensitivity to a Higgs boson produced by vector boson fusion. We find no evidence of the Higgs boson and place limits on the Higgs boson production cross-section for Higgs boson masses between $100\,\mathrm{GeV}/c^2$ and $150\,\mathrm{GeV}/c^2$ at 95% confidence level. For a Higgs boson mass of $120\,\mathrm{GeV}/c^2$ the observed (expected) limit is 10.5 (20.0) times the predicted Standard Model cross-section.

The Higgs boson remains the only undiscovered particle of the standard model (SM) of particle physics. It is the physical manifestation of the mechanism which provides mass to fundamental particles [1, 2]. Direct searches at the LEP collider have excluded a Higgs boson mass $m_H < 114.4\,\mathrm{GeV}/c^2$ at 95% confidence level (CL) [3], while the Tevatron has excluded a Higgs boson mass between $163\,\mathrm{GeV}/c^2$ and $166\,\mathrm{GeV}/c^2$ at 95% CL [4]. The Tevatron has reported a preliminary update which extends the exclusion region for a Higgs boson mass between 158 and $175\,\mathrm{GeV}/c^2$. [5]. Global fits to precision electroweak measurements set a one-sided 95% CL upper limit on m_H at $157\,\mathrm{GeV}/c^2$ [6].

This Letter presents the results of a search for the Higgs boson using an integrated luminosity of $4\,\mathrm{fb}^{-1}$ of $p\bar{p}$ collision data at $\sqrt{s} = 1.96\,\mathrm{TeV}$ recorded by the Collider Detector at Fermilab (CDF II). We search for a Higgs boson decaying to a pair of bottom-quark jets ($b\bar{b}$) accompanied by two additional quark jets (qq'). This search is most sensitive to a Higgs boson with low mass, $m_H < 135\,\mathrm{GeV}/c^2$, where the Higgs boson decay to $b\bar{b}$ is dominant [7]. The two production channels studied are associated production and vector boson fusion (VBF). The associated production channel is $p\bar{p} \to VH \to qq'\,b\bar{b}$, where V is a W/Z vector boson, which decays to a pair of quarks. The hadronic branching ratio of V to qq' is $\simeq 70\%$ [8]. In the VBF channel, $p\bar{p} \to qq'H \to qq'\,b\bar{b}$, the incoming partons each radiate a V and the two V fuse to form a Higgs boson.

Low-mass Higgs boson searches at CDF have concentrated on signatures that are a combination of jets, leptons and missing transverse energy which help to constrain the backgrounds but the signal yields are small [9–11]. The hadronic modes used in this search exploit the larger branching ratio and thus have the largest signal yields among all the search channels at CDF. The major

challenge for this search is the modeling and suppression of the large background from QCD multijets.

A previous Letter on the search for the Higgs boson in the all-hadronic channel was published using an integrated luminosity of $2\,\mathrm{fb}^{-1}$ [12]. This Letter has improved the analysis sensitivity by a factor of two: a factor of $\approx \sqrt{2}$ from doubling the analyzed data and a factor of 1.4 from improvements to the analysis which are discussed in this Letter.

The CDF II detector is an azimuthally and forward-backward symmetric detector designed to study $p\bar{p}$ collisions and described in detail in [13–15] and references therein. Jets are defined by a cluster of energy in the calorimeter deposited inside a cone of radius $\Delta R = \sqrt{\Delta\phi^2 + \Delta\eta^2} = 0.4$ [16] as reconstructed by the JetClu algorithm [17]. Corrections are applied to the measured jet energy to account for detector calibrations, multiple interactions, underlying event and energy outside of the jet cone [18].

The data for this search were selected by two multijet triggers. The first $2.8\,\mathrm{fb}^{-1}$ used a trigger which selected four jet clusters with energy of at least 15 GeV and total transverse energy $> 175\,\mathrm{GeV}$. This trigger was used in the previous result [12]. The remaining $1.1\,\mathrm{fb}^{-1}$ was recorded with a new trigger which selected three jet clusters with energy of at least 20 GeV and total transverse energy $> 130\,\mathrm{GeV}$. The new trigger improves the acceptance for low-mass Higgs by a factor of two.

After offline reconstruction, we select events with four or five jets where each jet has $E_T > 15\,\mathrm{GeV}$ and $|\eta| < 2.4$. The selected jets are ordered by descending jet-E_T and any fifth jet plays no further role in the search. The scalar sum of the four leading jets is required to be $> 220\,\mathrm{GeV}$. Events with isolated leptons or missing transverse energy significance [19] > 6 are removed to suppress the $t\bar{t}$ background.

The next stage of offline selection requires exactly two of the four leading jets to be identified ("tagged") as bottom-quark jets (b jet). A b jet is identified by its displaced vertex, as defined by the SecVtx algorithm [14], or by determining the tracks within the jet are unlikely to have originated from the primary $p\bar{p}$ collision as defined by the JetProb algorithm [20].

The two b-tagging algorithms are combined to form two non-overlapping b-tagging categories: SS when both jets are tagged by SecVtx, SJ when one jet is tagged by SecVtx and the other by JetProb. For a jet tagged by both algorithms, SecVtx takes precedence as it has a lower rate of misidentifying a light flavor jet as a b jet. The previous $2\,\mathrm{fb}^{-1}$ search only included the SS category [12]. The addition of the SJ category increased the signal acceptance by 36%. Other b-tagging combinations, such as both b jets selected by JetProb, were not considered in this search as the relative gain in the background is much larger than that for the signal.

The events which pass the offline selection are separated into VH or VBF signal regions. Both signal regions are defined by the invariant masses of the two b-tagged jets, m_{bb}, and the remaining leading two q-jets, m_{qq}. The division of events is based on the different kinematics of the two processes. The VH channel has two mass resonances: m_{bb} from the Higgs boson decay and m_{qq} from the V decay. The VH signal region is defined as $75 < m_{bb} < 175\,\mathrm{GeV}/c^2$ and $50 < m_{qq} < 120\,\mathrm{GeV}/c^2$. The VBF channel shares the same m_{bb} Higgs boson mass resonance but there is no accompanying resonance for m_{qq}. When compared to the background, a cut requiring $m_{qq} > 120\,\mathrm{GeV}/c^2$ optimizes the VBF signal over background ratio which exploits the large $\Delta\eta$ between the q-jet pair. The VBF signal region is defined as $75 < m_{bb} < 175\,\mathrm{GeV}/c^2$ and $m_{qq} > 120\,\mathrm{GeV}/c^2$. The division of the events by their b-tagging categories and their signal regions gives four analysis channels: VH-SS; VH-SJ; VBF-SS; VBF-SJ.

The VH and VBF production are modeled with pythia [21] combined with a geant-based [22] simulation of the CDF II detector [23]. The background is dominated by QCD production of multi-jets which is modeled by a data-driven technique developed in [12] and described in more detail below. The non-QCD backgrounds are modeled by simulation normalized to next-to-leading order cross sections and are described in detail in [12]. After applying the selection criteria and correcting for the simulated trigger efficiency [12], the expected yields for a Higgs boson of mass of $120\,\mathrm{GeV}/c^2$ for the VH and VBF signal regions are 7.8(SS)/2.9(SJ) and 3.2(SS)/1.2(SJ) events. The total background for the VH and VBF signal regions are about 17000(SS)/9300(SJ) and 18000(SS)/9500(SJ) events. The background composition is ∼98% QCD and the remaining 2% is a mixture of $t\bar{t}$, Z+jets, single-top, W+jets and diboson events. We estimate the contributions of these backgrounds in the same way as in [12].

The large background precludes the use of simple variables, such as the dijet mass, to search for a Higgs boson signal. We use an artificial neural network (NN) from the tmva package [24] to separate Higgs boson signal events from the dominant QCD background and trained at Higgs masses of 100, 120 and $140\,\mathrm{GeV}/c^2$. As the kinematics for VH and VBF Higgs signals are different, a dedicated NN for each signal is trained. The input variables for the VH neural net are m_{bb}, m_{qq}, the jet shapes (explained below) of both q-jets, the cosine of the helicity angle $\cos\theta^*_{q_1}$ [25], the cosine of the leading jet scattering angle in the four jet rest frame $\cos\theta_3$ [26] and χ which is a measure of whether both the b-jet pair and q-jet pair are from a Higgs boson and V decay respectively. χ is defined as the minimum of χ_W and χ_Z where χ_W is defined as $\chi_W = \sqrt{(M_W - M_{qq})^2 + (M_H - M_{bb})^2}$ and a similar expression exists for χ_Z. For the VBF channel, the neural net inputs are m_{bb}, m_{qq} and the jet shape of both q-jets. As the kinematics are not affected by the

different b-tagging categories, the neural net is trained with SS data as it has a better signal/background ratio. The NN distribution for the VH-SS channel, trained on simulated 120 GeV/c^2 Higgs boson events, is shown in Fig. 1. The NN returns a more negative (positive) score for background (signal) events.

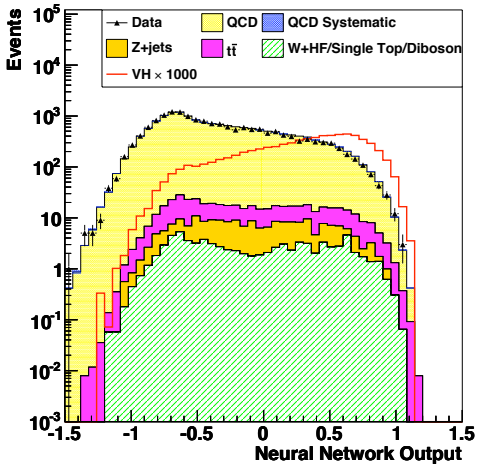

FIG. 1: NN distribution for VH-SS trained on simulated 120 GeV/c^2 Higgs Boson events.

The QCD multi-jet background consists of a mixture of quark and gluon jets while the Higgs signal jets are mostly quark jets. One can make use of the fact that the gluon jets tend to be broader than light flavor quark jets to help separate the Higgs signal from the QCD multi-jet background [27]. The width of a jet is characterized by the jet ϕ-moment $\langle\phi\rangle$ and jet η-moment $\langle\eta\rangle$ [28]. $\langle\phi\rangle$ is defined by Eq.(1) where the summation for the jet-moments are over the calorimeter towers used to form the jets and uses the tower-E_T ($E_t^{\rm tower}$), the jet-E_T ($E_t^{\rm jet}$), the tower's ϕ position ($\phi_{\rm tower}$) and the jet's ϕ position ($\phi_{\rm jet}$). A similar definition exists for $\langle\eta\rangle$.

$$\langle\phi\rangle = \sqrt{\sum_{\rm towers}\left[\frac{E_t^{\rm tower}}{E_t^{\rm jet}}\left(\Delta\phi(\phi_{\rm tower},\phi_{\rm jet})\right)^2\right]} \qquad (1)$$

The jet-width depends not only on the parton initiating the jet but also the jet-E_T, jet-η and the number of reconstructed primary vertices. The variation of the jet-width measurement by these variables is removed by parameterizing their dependence and rescaling the jet-moment to a common reference value of jet-E_T=50 GeV, jet-η=0 and one reconstructed vertex.

The simulation of the jet shapes was verified using events from $t\bar{t} \to b\ell\nu + bqq'$, where ℓ are electrons or muons, as this provides a source of light-flavor quark jets in data. The event selection from [29] was used to select a data sample which is dominated by $t\bar{t}$ ($\sim 86\%$) followed by W+jets, Z+jets, single top, diboson and backgrounds where light-flavor jets are misidentified as b jets. The two highest E_T untagged jets in the event whose dijet mass is consistent with a W boson ($M_W = 80 \pm 30$ GeV/c^2) are assumed to be quark jets. The jet shapes of these quark jets are compared to a simulation sample of $t\bar{t}$ and W+jets in the same fraction as measured in data. An offset of +0.0024 (+0.0015) was added to the simulation's η-moment (ϕ-moment) to agree with data. Half of the offset values were assigned as systematic uncertainties for the jet η and ϕ-moment. A cross-check using Z+jets simulation and data was performed and found to agree only after applying the corrections derived from $t\bar{t}$.

The parameterizations used to rescale the jet-width to the common reference point for the simulation were cross-checked with the Higgs boson sample. The rescaled jet-widths for VH were consistent with $t\bar{t}$. However the rescaled jet-widths for VBF were lower than $t\bar{t}$. This difference was considered as an additional systematic uncertainty for the VBF jet-width. Half of this maximum difference was used as a measure of the uncertainty: $\pm$0.0025 ($\pm$0.0010) for the VBF jet $\langle\eta\rangle(\langle\phi\rangle)$.

A data-driven method, known as the tag rate function (TRF), is used to model the dominant QCD multijet background. The TRF is applied to events with at least one b-tagged jet (single tagged events) to predict the distribution of events with exactly two b-tagged jets (double tagged events). For each single-tagged event, the TRF gives the probability of each additional jet, called a *probe* jet, to be a second b-tagged jet. The TRF is described in detail in [12]. In this search the TRF was parameterized as a function of three variables: the probe jet-E_T, probe jet-η and ΔR between the tagged b jet and probe jet. The TRF is measured using jets in the TAG region (Fig. 2), defined as $m_{qq} < 45$ GeV/c^2, $m_{bb} < 50$ GeV/c^2 and $m_{bb} > 200$ GeV/c^2. The TRF is then applied to the single tagged events in the VH and VBF signal regions to predict the double tagged events.

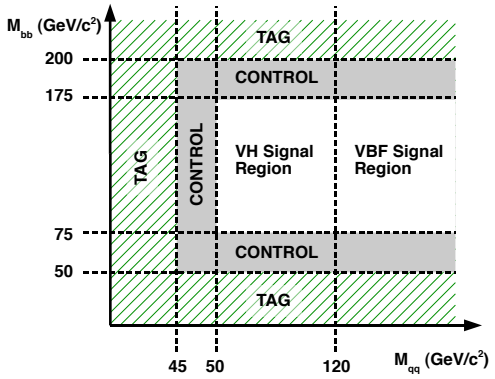

FIG. 2: $m_{bb} - m_{qq}$ plane: This plane illustrates the regions used for the VH,VBF signal and the TRF.

The TRF predictions were verified by comparing the shapes of different variables constructed from single-

tagged events, after applying the TRF, and double tagged events from the TAG region. The TRF was able to model the shapes of all the NN training variables except m_{qq} and the jet shapes $\langle\phi\rangle$ and $\langle\eta\rangle$ which required their own corrections. The prediction for these variables were scaled by the ratio of their observed shape to their prediction in the TAG region. These scaling corrections are applied in the VH and VBF signal regions when predicting the shapes of double tagged events.

We consider two sources of systematic uncertainty on the shape of the NN output distributions for the multijet background. The interpolation uncertainty accounts for possible difference in the TRF between the regions where it was measured (TAG) and applied (SIGNAL). An alternative TRF was measured using events in the CONTROL region, as indicated in Fig. 2, which is still background-dominated. The difference in the shapes of the predicted background distribution in the NN output for the two TRFs is treated as a systematic uncertainty. The second source is due to the uncertainty in applying the m_{qq} and jet shapes scaling factors measured in the TAG region to the SIGNAL region. Alternative scaling factors were derived using events in the CONTROL region.

The systematic uncertainties which affect the acceptance of the Higgs signal and non-QCD backgrounds are: $\pm7\%$ jet energy scale uncertainty [18], $\pm2\%$ parton distribution function uncertainty, b-tagging scale factor between simulation and data ($\pm7.6\%$ SS / $\pm9.7\%$ SJ), $\pm2\%$ VH / $\pm3\%$ VBF initial- and final-state radiation (ISR/FSR) uncertainties for the signal , $\pm4\%$ trigger acceptance uncertainty and $\pm6\%$ luminosity uncertainty [5]. The uncertainty on the cross-sections for the non-QCD backgrounds are: $\pm10\%$ for $t\bar{t}$ and single-top [5] , $\pm6\%$ for diboson [5],$\pm50\%$ for W+jets and Z+jets. In addition to changes to the acceptance, changes to the shape of the NN output were considered for the Higgs boson signal. The uncertainties which affected the shape of the NN output were jet-energy scale, ISR/FSR and jet-width. It should be noted the dominant systematic error for this analysis came from the uncertainties of the QCD prediction.

When the data are compared to the background prediction, we find no excess of events over the expected background and set upper limits on the excluded Higgs boson cross-section at 95% CL for $100 < m_H < 150\,\mathrm{GeV}/c^2$. The limits are calculated using a Bayesian likelihood method with a flat prior for the signal cross-section and Gaussian priors for the uncertainties on acceptances and backgrounds [30]. The normalization of the multijet background is a free parameter that is fit to the data. We combine the four search channels by taking the products of their likelihoods and simultaneously varying their systematic uncertainties.

For $m_H = 120\,\mathrm{GeV}/c^2$, the observed (expected) limit, normalized to the SM prediction, for the individual analysis channels are 11.9(25.6) for VH-SS, 43.4(51.8) for VH-SJ, 47.0(49.4) for VBF-SS, 93.7(132.3) for VBF-SJ, and 10.5(20.0) for the combination. The combined channel limits for Higgs boson masses in the range between 100 - $150\,\mathrm{GeV}/c^2$ are shown Fig. 3.

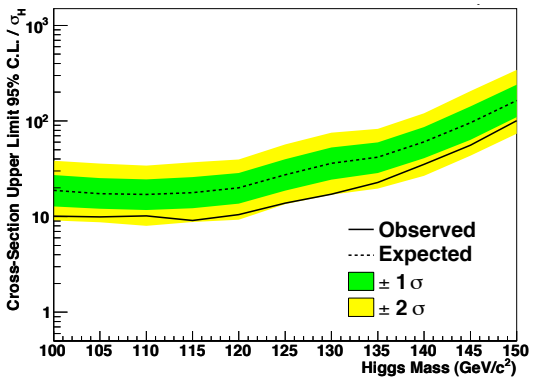

FIG. 3: Expected (dashed) and observed (solid) 95% CL normalized to the SM cross-section for the combined VH and VBF channel. The dark (light) band represents the $1\sigma(2\sigma)$ expected limit range.

The observed limits for the individual search channels are in agreement with their expected limits except for the VH-SS channel where there is a deficit in the data in the high signal region of the NN. As the VH-SS channel is the most sensitive, it has the strongest influence on the combined limit. Figure 4 shows the ratio of the data to background for the four analysis channels for a NN trained on a $120\,\mathrm{GeV}/c^2$ Higgs boson simulated data. All four channels show a ratio ≈ 1 over the whole NN output range, but the VH-SS channel has several points with a ratio of ≈ 0.9 about a NN output of 0.5; the high signal region of NN output. The same TRF is used in the VBF-SS channel and the same NN is used in the VH-SJ channel, neither of which show such a feature. The low ratio for VH-SS is likely a statistical fluctuation rather than evidence of background mismodeling.

In summary, the measurement presented in this Letter shows a factor of two improvement over the previous $2\,\mathrm{fb}^{-1}$ result for the all-hadronic Higgs search [12] . This Letter extends the $2\,\mathrm{fb}^{-1}$ analysis by including the VBF channel, adding an additional algorithm to identify bottom-quark jets, adding an artificial neural network to separate signal from background which includes jet shapes to distinguish gluons from quark jets, and by doubling the analyzed data set. As the Tevatron continues to collect more data and further improvements to the analysis technique will extend the sensitivity of the all-hadronic Higgs search.

We thank the Fermilab staff and the technical staffs of the participating institutions for their vital contributions. This work was supported by the U.S. Department of Energy and National Science Foundation; the Italian

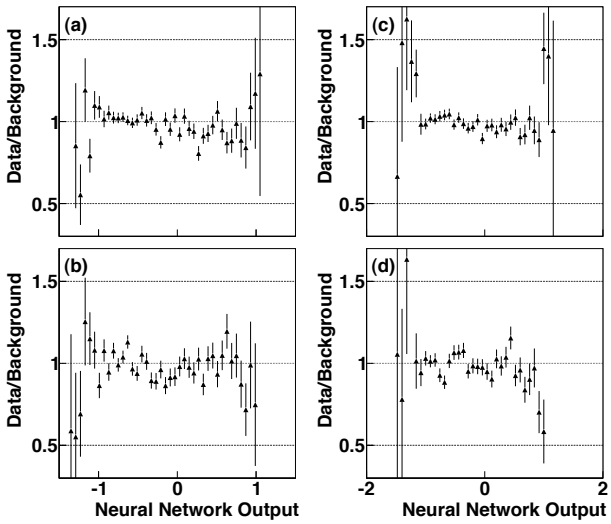

FIG. 4: Ratios of the data to background for VH-SS (a), VH-SJ (b), VBF-SS (c), and VBF-SJ (d) for the NN trained on 120 GeV/c^2 Higgs boson simulated events.

Istituto Nazionale di Fisica Nucleare; the Ministry of Education, Culture, Sports, Science and Technology of Japan; the Natural Sciences and Engineering Research Council of Canada; the National Science Council of the Republic of China; the Swiss National Science Foundation; the A.P. Sloan Foundation; the Bundesministerium für Bildung und Forschung, Germany; the World Class University Program, the National Research Foundation of Korea; the Science and Technology Facilities Council and the Royal Society, UK; the Institut National de Physique Nucleaire et Physique des Particules/CNRS; the Russian Foundation for Basic Research; the Ministerio de Ciencia e Innovación, and Programa Consolider-Ingenio 2010, Spain; the Slovak R&D Agency; and the Academy of Finland

[1] P. W. Higgs, Phys. Lett., **12**, 132 (1964).
[2] F. Englert, Phys. Rev. Lett., **13**, 321 (1964).
[3] The ALEPH, DELPHI, L3 and OPAL Collaborations, and the LEP Working Group for Higgs boson searches, Phys. Lett. B, **565**, 61 (2003).
[4] T. Aaltonen *et al.* (CDF Collaboration), Phys. Rev. Lett., **104**, 061802 (2010).
[5] CDF Collaboration and D0 Collaboration and Tevatron New Physics and Higgs Working Group, "Combined CDF and D0 upper limits on standard model higgs-boson production with up to 6.7 fb^{-1} of data," arXiv:hep-ex/1007.4587v1.
[6] ALEPH, CDF, D0, DELPHI, L3, OPAL, SLD, the LEP Electroweak Working Group, the Tevatron Electroweak Working Group, and the SLD Electroweak and Heavy Flavor Working Groups, "Precision Electroweak Measurements and Constraints on the Standard Model," arXiv:hep-ex/0911.2604.
[7] A. Djouadi, J. Kalinowski, and M. Spira, Comput. Phys. Commun., **108**, 56 (1998).
[8] C. Amsler *et al.*, Phys. Lett. B, **667**, 1 (2008).
[9] T. Aaltonen *et al.* (CDF Collaboration), Phys. Rev. D, **80**, 071101 (2009).
[10] T. Aaltonen *et al.* (CDF Collaboration), Phys. Rev. Lett., **103**, 101802 (2009).
[11] T. Aaltonen *et al.* (CDF Collaboration), Phys. Rev. Lett., **104**, 141801 (2010).
[12] T. Aaltonen *et al.* (CDF Collaboration), Phys. Rev. Lett., **103**, 221801 (2009).
[13] D. E. Acosta *et al.* (CDF Collaboration), Phys. Rev. D, **71**, 032001 (2005).
[14] D. E. Acosta *et al.* (CDF Collaboration), Phys. Rev. D, **71**, 052003 (2005).
[15] A. Abulencia *et al.* (CDF Collaboration), J. Phys. G, **34**, 2457 (2007).
[16] CDF uses a cylindrical coordinate system with the z axis aligned along the proton beam direction, θ is the polar angle relative to the z-axis and ϕ is the azimuthal angle. The pseudorapidity is $\eta \equiv -\ln(\tan\theta/2)$. The transverse energy is $E_T \equiv E\sin\theta$.
[17] F. Abe *et al.* (CDF Collaboration), Phys. Rev. D, **45**, 1448 (1992).
[18] A. Bhatti *et al.* (CDF Collaboration), Nucl. Instrum. Methods, **A566**, 375 (2006).
[19] Missing transverse energy significance is the ratio of the total missing transverse energy to the total transverse energy.
[20] A. Abulencia *et al.* (CDF Collaboration), Phys. Rev. D, **74**, 072006 (2006).
[21] T. Sjostrand *et al.*, Comput. Phys. Commun., **135**, 238 (2001).
[22] R. Brun *et al.*, CERN-DD-EE-84-01 (1987).
[23] E. Gerchtein and M. Paulini, arXiv:hep-ex/0306031.
[24] A. Hoecker *et al.*, arXiv:hep-ex/0703039v5.
[25] $\cos\theta^*_{q_1}$ is the cosine helicity angle of the leading non b jet (q_1). The helicity angle $\theta^*_{q_1}$ of the leading non b jet q_1 is defined to be the angle between the momentum of q_1 in the $q_1 - q_2$ rest frame and the total momentum of $q_1 - q_2$ in the lab frame.
[26] $\cos\theta_3$ is defined in a three jet rest frame as the cosine of the leading jet scattering angle. We reduce from four jets to three jets by combining the two jets with the lowest two jet mass. Thus $\cos\theta_3 = \frac{\vec{P_{AV}}\cdot\vec{P_3}}{|\vec{P_{AV}}||\vec{P_3}|}$ where $\vec{P_3}$ is the third jet and $\vec{P_{AV}}$ is the vector sum of the three jets in the lab frame [31].
[27] D. Acosta *et al.* (CDF Collaboration), Phys. Rev. D, **71**, 112002 (2005).
[28] T. Aaltonen *et al.* (CDF Collaboration), Phys. Rev. D, **81**, 052011 (2010).
[29] T. Aaltonen *et al.* (CDF Collaboration), Phys. Rev. Lett., **105**, 012001 (2010).
[30] J. Heinrich *et al.*, arXiv:physics/0409129v1.
[31] S. Geer and T. Asakawa, Phys. Rev., **D53**, 4793 (1996).